The Holocene 12,3 (2002) pp. 267–277

1300 years of climatic history for Western Central Asia inferred from tree-rings

Jan Esper,[1*] Fritz H. Schweingruber[1] and Matthias Winiger[2]

([1]Swiss Federal Institute of Forest, Snow and Landscape Research (WSL), Zürcherstrasse 111, 8903 Birmensdorf, Switzerland; [2]Department of Geography, University of Bonn, Meckenheimer Allee 166, 53115 Bonn, Germany)

Received 18 November 2000; revised manuscript accepted 12 November 2001

A HOLOCENE RESEARCH PAPER

Abstract: More than 200 000 ring-width measurements from 384 trees were obtained for 20 individual sites ranging from the lower to upper local timber-lines in the Northwest Karakorum of Pakistan and the Southern Tien Shan of Kirghizia. Samples were obtained predominantly from juniper species (*Juniperus*) and were analysed to reconstruct regional climatic variation patterns in Western Central Asia since AD 618. Site distribution represents diverse ecological conditions (e.g., combinations of temperature and moisture stress) within the Karakorum and Tien Shan mountains, permitting both intra-montane and inter-montane comparisons of chronologies. Three different types of chronologies reflecting interannual-, decadal- and centennial-scale ring-width variations were calculated: a statistic skeleton-plotting technique was used to identify ring-width pointer years (interannual); a 101-year kernel filter was used to identify decadal-scale variations; and, for a subset of long-lived trees, the mean ring-width of the entire single series was used to identify centennial trends. After extracting and calibrating each of these three distinct wavelengths in ring-width variation, the results were combined into a comprehensive reconstruction reflecting primarily temperature fluctuations in Western Central Asia since AD 618. The nature and the temporally changing strength of the climatic signals of this reconstruction are discussed in detail. A maximum latewood density record of *Pinus tienschanica* from Central Tien Shan was used as a predictor series to calibrate and validate tree-ring-width variation. In so doing, we link our results to the circumpolar maximum latewood-density network (Briffa *et al.*, 1998a; 1998b; Schweingruber and Briffa, 1996).

Key words: Tree-rings, dendrochronology, climate variability, *Juniperus*, Western Central Asia, Karakorum, Tien Shan.

Introduction

The significance of reconstructing past climatic variability patterns, prior to the instrumental period, is widely appreciated in the current debate on distinguishing natural and anthropogenic climate change (e.g., Briffa and Osborn, 1999; Jones *et al.*, 1996; Mann *et al.*, 1998). In contrast to other, more localized high-resolution proxy climate records (e.g., high-latitude and high-elevation ice cores), tree-ring chronologies can be derived from much of the middle- to high-latitude landmasses (Dean *et al.*, 1996; Schweingruber, 1996). Comparisons of different, independently developed, mean tree-ring chronologies yield additional validation of reconstructed climatic signals (e.g., Bräuning, 1994; 1999; La Marche, 1974). High-elevation alpine ecosystems, which are of particular interest in this study, are important regions for detecting the patterns of climatic change on regional scales. High mountain regions are exceptionally sensitive to climatic variations and conspicuous interactions exist between these ecosystems and climate (Barnett *et al.*, 1988; Ives and Messerli, 1989; Shiyatov, 1993).

The aim of this work is to determine the frequency of climatically forced extreme years and the magnitude of decadal to centennial timescale variations in the mountains of Western Central Asia since AD 618. Collections of tree-ring-width (TRW) chronologies from 20 sites, located in the Northwest Karakorum and Southern Tien Shan regions, were used to answer the following questions:

- What is the strength and nature of climatic signals in tree-ring data on multiple timescales?
- What differences in climatic response may be attributed to vertical ecological gradients in several valleys within the Karakorum (intra-montane comparison)?
- What supraregional climatic signals are common to both the Karakorum and Tien Shan mountains (inter-montane comparison)?

*Author for correspondence (e-mail: esper@wsl.ch)

 10.1191/0959683602hl543rp

Material

The reconstruction of the variation of climatic patterns in the Western Central Asia sector was based on analyses of more than 200 000 TRW values from 20 sites (mostly juniper species) in the Northwest Karakorum, Pakistan, and the Southern Tien Shan, Kirghizia (Figure 1). A maximum latewood density (MXD) chronology of *Picea tienschanica* Rupr. from a site located in the Central Tien Shan (41°40′N/76°26′E) near Narin supplements the analysis. Even though the distance between the Northwest Karakorum (35–37°N/74–76°E) and Southern Tien Shan (40°10′N/72°35′E) is only 500 km, very distinct and different synoptic weather patterns have been described for each region (see Böhner, 1996, and references therein). Sites in the Northwest Karakorum are affected by westerlies, as well as monsoonal depressions. By contrast, sites in the Southern Tien Shan are influenced by a strongly continental climate, without precipitation transport from the Arabian Sea. The study regions are separated by the main Karakorum mountain range, the Western Hindu Kush and the Pamirs (Flohn, 1958; Reimers, 1992; Schweinfurth, 1956; Troll, 1952; Weiers, 1995; 1998).

Fifteen TRW sites were sampled from four valleys (Table 1, P1–P4) in the Northwest Karakorum and five juniper TRW sites were sampled in the Karagui valley (K1), Southern Tien Shan. 'Sites' represent areas of ecologically homogenous conditions, similar aspect and slope. P5 (Table 1) is a collection of trees sampled along the Hunza valley. The juniper chronologies are composed by *Juniperus turkestanica* Kom., *Juniperus seravchanica* Komarov. and *Juniperus semiglobosa* Regel (Nüsser, 1998; Schickhoff, 1993; 1995). In the Bagrot valley (P1) *Pinus wallichiana* A.B. Jackson and *Picea smithiana* (Wallich) Boiss. were sampled in addition to the junipers. Within most valleys (Table 1, Karagui K1, Bagrot P1, Chaprot P2 and Satpara P4) the sites range from the lower arid to the upper humid timber-lines. Such selection enabled the comparison of climatic signals from sites predominantly moisture-stressed with sites predominantly temperature-stressed. Two cores were taken from each tree in stands with homogenous species composition and vegetation structure, and, whenever possible, only minimal apparent human impact.

Population density and tree growth-forms of the junipers are comparable to that described for bristlecone pine from the White Mountains of southwestern USA (Ferguson, 1968; Fritts, 1969; Graybill and Idso, 1993; Kelly *et al.*, 1992; Wright and Mooney, 1965). Distances between single standing trees often exceed 10 m. Cross-sections of juniper trees are star-shaped and old individuals develop strip-bark growth-forms. In some cases, the cambial die-back is so pronounced that only a narrow strip on the stem is still active (Esper 2000a; 2000b). Characteristics of population density, as well as growth forms of junipers, were evaluated to aid in the interpretation of TRW variations expressed particularly on the centennial scale (see below).

Methods

There is general agreement on the standards a mean chronology should meet for reconstructing climatic variability (Fritts, 1976). One essential requirement is that a composite site chronology must express some common variance among all trees from the same site (Briffa and Jones, 1990; Esper *et al.*, 2001; Wigley *et al.*, 1984). To maximize the common variance in chronologies, standardization is necessary. In this case, expected growth curves are fitted to the original single TRW series in order to calculate either ratios or residuals of raw ring-widths (Bräker, 1981; Cook and Briffa, 1990; Cook *et al.*, 1990). Esper (2000a), however, stated that only one fitting-model should be applied in the process of standardization to calculate a chronology from different trees at one site. If, nevertheless, different growth curves are fitted to individual trees from the same site (e.g., a negative exponential curve fitted to a TRW series that shows a long-term, age-related negative trend, and a straight line with no slope fitted to another TRW series that shows a long-term positive trend), the standardization may lead to an overestimation of positive long-term trends, particularly in the twentieth century. This artifact is a result of detrending age-related *and* climate-related negative trends in the early periods of a chronology – perhaps reflecting the transition from the 'Mediaeval Warm Period' into the 'Little Ice Age' – and not detrending climate-related positive trends in the modern period. Reconstructions of this kind are of limited value in understanding centennial trends, particularly during the early periods of the chronologies, where any low-frequency variation has been removed.

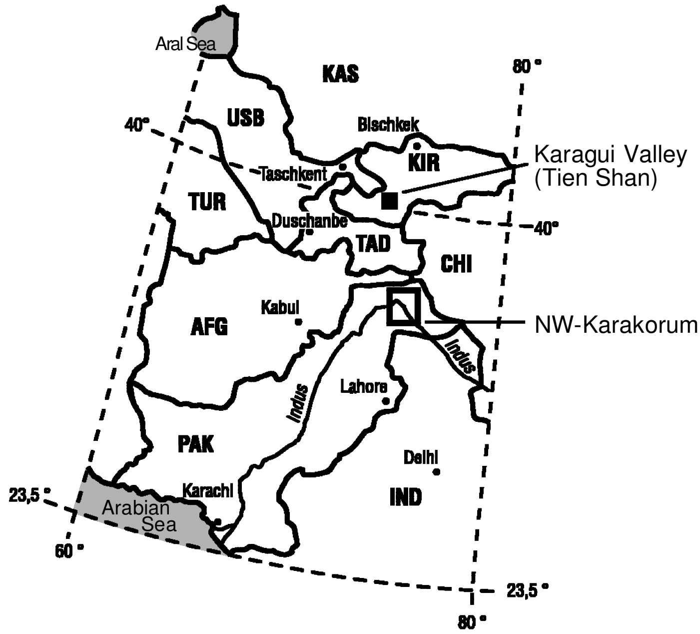

Figure 1 Western Central Asia region and investigated study areas in the Tien Shan and the Karakorum.

Table 1 Western Central Asia tree-ring chronologies

Chrono.	Elev./exp./incl.	No. trees	Max. age/aver. age (yr.)	Aver. width (mm)	Interser. GLK (%)*	Coeff. of var.*
K1a	3200 m/SW/20°	30	AD 1316/346	0.39	61	0.31
K1b	3000 m/SSW/20°	25	AD 1157/422	0.42	59	0.31
K1c	2900 m/N/25°	20	AD 1346/326	0.52	59	0.28
K1d	2900 m/SSW/50°	18	AD 1591/221	0.53	58	0.32
K1e	2800 m/W/20°	43	AD 1378/227	0.62	58	0.33
P1a	3100 m/NNW/31°	26	AD 1535/189	1.36	64	0.32
P1b	3300 m/NNW/33°	19	AD 1369/268	0.78	62	0.22
P1c	3050 m/S/35°	21	AD 1438/236	1.00	65	0.32
P1d	3750 m/S/42°	17	AD 1240/218	1.04	59	0.23
P2a	2700 m/S/31°	24	AD 1587/173	0.75	64	0.36
P2b	3500 m/S/40°	19	AD 1032/481	0.47	64	0.27
P2c	3900 m/S/47°	11	AD 1144/459	0.33	62	0.29
P3a	3900 m/SW/30°	13	AD 476/517	0.50	64	0.28
P3b	3800 m/ENE/30°	15	AD 968/510	0.31	66	0.27
P3c	3600 m/ENE/20°	20	AD 554/632	0.33	73	0.32
P3d	3900 m/SSE/22°	18	AD 1069/398	0.35	64	0.30
P4a	3300 m/NW/45°	13	AD 1412/343	0.64	59	0.27
P4b	3700 m/S/45°	18	AD 736/755	0.28	62	0.29
P4c	3900 m/S/48°	17	AD 388/581	0.29	66	0.23
P5	single trees	7	AD 568/774	0.36	61	0.28

*Result from averaging the individual Gleichläufigkeiten and coefficients of variation between all trees in each site

Scales of analysis

Three different types of site chronologies reflecting three distinct frequencies of TRW variations were calculated: interannual-, decadal- and centennial-scale variations. For each frequency, only one standardization model was applied to build chronologies. We recognise that each standardization procedure creates an average curve that differs in its temporal bias. For example, if centennial variability is present, then the mean chronology will have wider confidence limits than chronologies emphasizing variations on shorter timescales (Briffa *et al.*, 1996).

To emphasize extreme years (= pointer years, sensu Schweingruber *et al.*, 1990), indexed series were derived using a method developed by Cropper (1979). Residuals from a five-year moving average were calculated to eliminate the low-frequency signal. Each residual was then scaled, dividing it by the standard deviation of the local mean. This technique identifies locally extreme values. Extreme residuals during periods of high local variance were devalued, and extreme residuals in periods of low local variance were emphasized. The resulting scaled values were multiplied by 1000 to significantly distinguish them from the other two chronology types. Extreme values were calculated for every TRW series and can be averaged to build mean chronologies from a site or a region. They are comparable to results achieved by the skeleton-plot method, which also emphasizes pointer years (Schweingruber *et al.*, 1990).

To emphasize decadal-scale variations, a 101-year kernel filter (Gasser and Müller, 1984) was fitted to each TRW series. This filter is known to have no 'end-effect problems' that typically appear when using common filter techniques. Calculated ratios between the observed TRW and the model estimates produce indexed series with stable mean and adjusted variance. Any wavelength longer than 100 years is eliminated and decadal-scale variations are retained (Cook and Kairiukstis, 1990).

Compared to the determination of pointer years and decadal-scale variations, extraction of common centennial trends is more complex. Above all, it is not possible to reconstruct low-frequency variations on timescales longer than the entire series length (Cook *et al.*, 1995). Additionally, growth models describing regionally common age-related trends (e.g., regional curve standardization (RCS) Briffa *et al.*, 1995; 1996) or classical linear detrending models (LT) are not applicable to the Western Himalayan data. One reason for this is that the star-shaped growth form generally results in a lack of innermost rings on sampled cores. Estimates of the pith offset (difference between the innermost ring of a core sample and the pith of a tree) are generally needed to apply age-related standardization methods, such as RCS. Fitting constrained functions, such as LT, which have the ability to recover low-frequency signals, often cause serious 'end-effect problems', especially when the trees grew very slowly and the LTs declined below approximately 0.5 mm/yr (Cook and Peters, 1997). Since there is no strong 'spread–versus–level relationship' (Cook and Peters, 1997) in the Western Himalayan data, calculating residuals together with a power transformation using linear standardization methods also seemed inappropriate.

As an alternative, a mean 'average division' method (*ad*-index) was used to reconstruct centennial-scale variability from a subset of 17 *Juniperus turkestanica* trees, all of them over 1000 years old, from sites near the upper timber-line in the Northwest Karakorum. Each tree's annual TRW was divided by the average TRW calculated over all years. Resulting series express comparable variance and stable mean. This method is particularly useful, because the old junipers developed strip-bark growth forms, so that the annual stem biomass increase was not distributed around the entire stem, and thus noticeable long-term age-trends are missing. Besides, these trees are not affected by stand dynamics often associated with closed-canopy forests, which commonly introduce strong age-related growth trends in the first decades of a tree's life. Nevertheless, the first 100 years of each single series were not used if the innermost rings of a core seemed to be *near* to the pith of the tree; and the first 50 years were not used if the innermost rings seemed to be *far* from the pith. Additionally, we analysed centennial-scale variations by developing normalized and kernel filtered series of 97 trees that were over 500 years old. A comparison of overall positive and negative growth anomalies during distinct periods, since AD 900, provides an expression of long-term growth fluctuations.

Figure 2 illustrates the methods used to emphasize the distinct wavelengths within one long-lived *Juniperus turkestanica* tree. The original TRW series in the upper panel reaching back to AD 786 expresses variations of different wavelengths and amplitudes. Calculating the *ad*-indexed series (Figure 2b) emphasizes centennial trends represented by a kernel low-pass filter (bold curve). Decadal-scale variations are emphasized by fitting a 101-year kernel filter to the original TRW series and calculating ratios from the filter. Again, a kernel low-pass filter emphasizes the decadal-scale variations in the resulting series since AD 1700 (Figure 2c). In the lowest panel, for the period AD 1913–23, the extreme years 1917 and 1921 were identified using the method developed by Cropper (1979) (Figure 2d).

Signal strength

To analyse the common underlying signal of chronologies, we used the interseries Gleichläufigkeit (sign test), which calculates the numbers of synchronous growth intervals from year to year between the single series, and the coefficient of variation (Table 1) (details in Esper *et al.*, 2001). Results of interseries Gleichläufigkeit indicate that most sites reach high degrees of common variance, measured in the high-frequency domain. The coefficient of variation was applied in a way to calculate the vertical spread between the single series contributing to a chronology (Esper *et al.*, 2001). Thus it quantifies levels of uncertainty within a chronology considering also the low-frequency domain. This parameter strongly depends on the type of model fitted to the series in the standardization procedure.

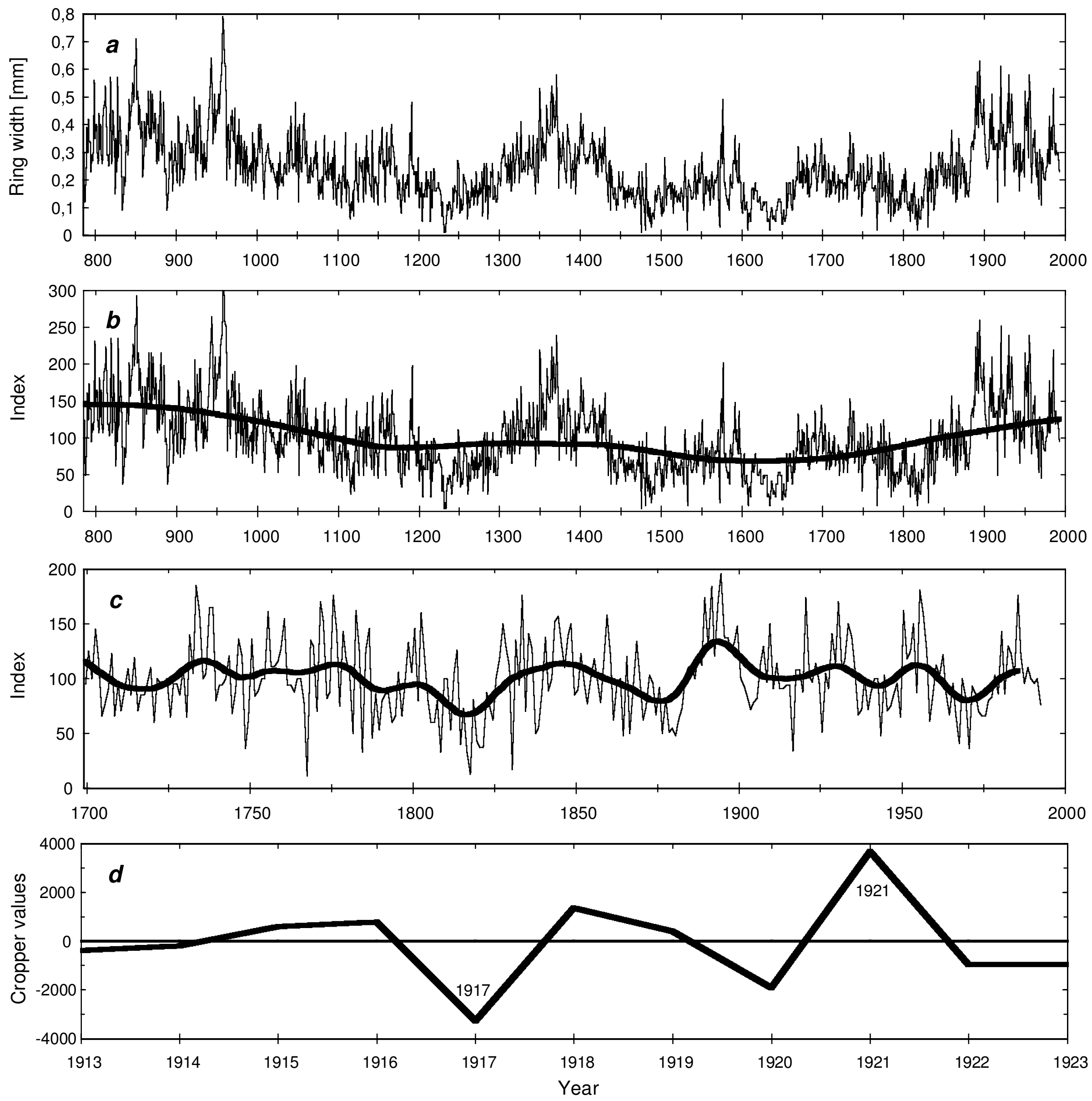

Figure 2 Example of separating independent frequencies from a TRW series of a single, long-lived *Juniperus turkestanica* tree (AD 786–1993) from site P4b. (a) Original TRW series. (b) Centennial trends emphasized by calculating ratios from the long-term average of the original TRW series. (c) Decadal-scale variations emphasized by calculating ratios from a 101-year kernel filter fitted to the original TRW series. (d) Event years calculated using a technique developed by Cropper (1979).

Table 1 presents the characteristics of the chronologies developed to emphasize decadal-scale variations (see example P3c illustrated in Figure 5a).

Transfer functions

Due to a lack of representative high-elevation meteorological stations in the Northwest Karakorum and Southern Tien Shan regions, the calibration of TRW variability in Western Central Asia is problematic. For this reason, we developed regional average curves of climate data from six meteorological stations (Gilgit, Lahore, Ludhiana, Murree, Peshawar and Simla) to calibrate TRW variations in the Karakorum region (Esper, 2000b). A MXD chronology of *Pinus tienschanica* from a site in Central Tien Shan, which is part of the high-latitude circumpolar MXD network (Briffa *et al.*, 1998a; 1998b; Schweingruber and Briffa, 1996; Vaganov *et al.*, 1999), was also used as a predictor to calibrate TRW variations in the Southern Tien Shan region. To suppress the influence of high-frequency variations, the recorded decadal TRW fluctuations were calibrated using filtered series (15-year moving average). All calibrations were carried out by the use of correlation coefficients with monthly or annual averages of temperature and precipitation. For the reconstruction of decadal temperature variations a simple linear regression was used.

Results

Chronology characteristics

The juniper chronologies are composed of *Juniperus turkestanica* Kom., *J. seravchanica* Komarov. and *J. semiglobosa* Regel. Descriptive statistics of TRW variations indicate no difference in growth between the species, as wood anatomical features of *J. turkestanica*, *J. seravchanica* and *J. semiglobosa* are identical (for details, see Esper, 2000b).

Average and maximum tree age influence the length and scales of potential climatic reconstructions (Cook *et al.*, 1995). Figure 3 illustrates the age structure of all trees sampled in the Tien Shan and Karakorum regions and the coherence between tree age and TRW for the entire data set. In both regions, trees between 100 and 400 years in age are well represented. The maximum series length in the Tien Shan is <900 years, whereas several junipers in the Karakorum are over 1000 years old (Figure 3a). A strong correlation between cambial age and TRW is recorded (Figure 3b). Trees younger than 500 years, particularly those less than 200 years, grew significantly faster than trees over 500 years. In the latter subset, average TRW varies only slightly. The recorded relation between cambial age and mean TRW indicates that the younger trees need to be standardized carefully before building mean chronologies.

Maximum and average series lengths (Table 1, Max. age/aver. age) are a result of limitations by climatic elements. This limitation is exceptionally strong at sites located near the upper timber-line and in valleys where precipitation is low. In the Karagui (K1a–K1e), Chaprot (P2a–P2c) and Satpara valleys (P4a–P4c), where sites range in elevation from the lower to the upper timber-lines, tree ages increase significantly with elevation. The oldest tree in the entire data set (AD 388) is a *Juniperus turkestanica* at P4c in the Satpara valley. The oldest sampled site, however, is P4b, in the same valley, 200 m below P4c. This observation indicates that tree selection influences the resulting age structure for each site as well. In the more humid Bagrot valley, where mixed stands of *Juniperus*, *Pinus* and *Picea* species were sampled (P1a, P1c), the age structure is more heterogeneous and the recorded differences are not site-dependent. Growth rate and age correlate again with recorded moisture, which decreases from Bagrot (P1) to Chaprot (P2) to Morkhun (P3) and Satpara (P4) in the Karakorum region. With decreasing humidity, the growth rate of the junipers decreases as the average age increases (Table 1).

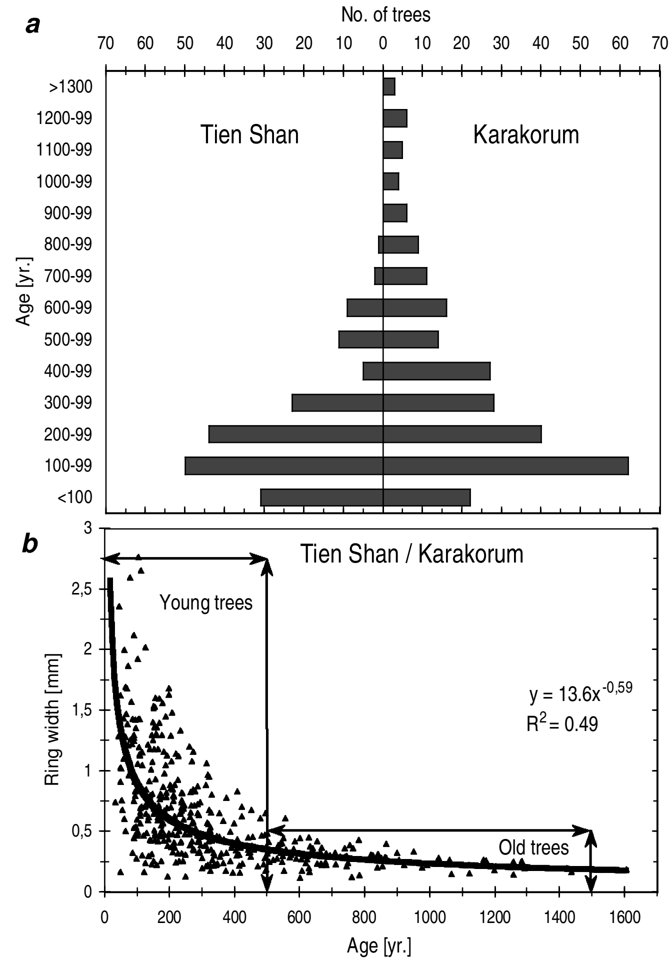

Figure 3 (a) Age structure. (b) Average TRW of single series versus age of single series.

Pointer years

Many of the observed pointer years, like AD 1917 (Figure 2), are represented in nearly all of the sites from the lower to the upper forest boundaries within the Karakorum and Tien Shan regions. Synchronous extreme years within the study areas were designated as regional pointer years. A portion of these regionally common years can be explained by temperature variation, while others were caused by precipitation variation (Esper, 2000b). This changing nature of the climatic signal needs to be considered when chronologies are calibrated (Schweingruber *et al.*, 1991).

Since most of the observed pointer years are identical between the two boundaries of forest distribution within the Karakorum and the Tien Shan, records of extreme growth reactions can easily be summarized. Two regional mean chronologies of pointer years, averaging 15 sites in the Karakorum and five sites in the Tien Shan, were developed. A comparison of these regional pointer-year records identifies supraregional extreme years that are synchronous across the Western Central Asia sector. This is despite the fact that the Tien Shan and the Karakorum are influenced by different synoptic climate systems.

The curve in Figure 4 illustrates the mean extreme ring-width values of Western Central Asia since AD 1400, obtained by averaging the regional records of the Karakorum and the Tien Shan. High values occur only if the trees in both regions record the same pointer year, e.g., 1917 (negative) or 1916 (positive), based on the criterion that a regional pointer year belongs to the 50 strongest since 1400 in the Karakorum *and* Tien Shan.

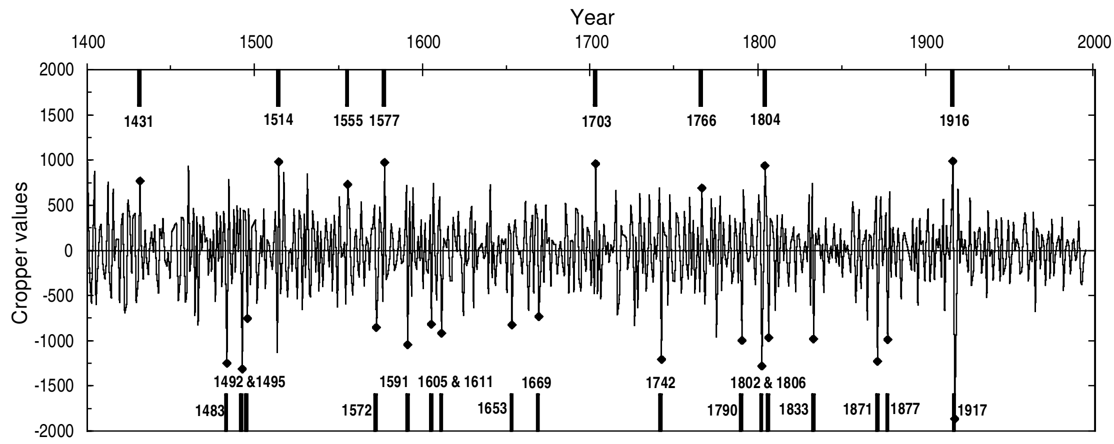

Figure 4 Supraregional pointer-year reconstruction in Western Central Asia since AD 1400. The curve indicates average extreme values from the Karakorum and the Tien Shan. Both regions have equal influence on the curve. At the bottom and the top, pointer years are labelled that are synchronous between both regions. Supraregional pointer years must be among the 50 highest values observed in both the Karakorum and the Tien Shan regions since 1400.

Synchronous (= supraregional) pointer years are marked by bold lines at the top (positive) and bottom (negative) of Figure 4. Taking into account that negative years are more common between the sites of one region, synchronous negative extremes appear more often ($n = 17$) than synchronous positive extremes ($n = 8$).

Decadal-scale variations

Significant differences in the strength of decadal-scale variations are related to site distribution. Common decadal-scale variations are exceptionally strong between the high-elevation sites above 3500 m a.s.l. in the Karakorum region. Comparable, but less synchronous, decadal-scale variations are observed between K1a, K1b and K1c in the Tien Shan region. This high-synchronicity permits the construction of regional mean chronologies from high-elevation sites, for comparison between the Karakorum and Tien Shan regions.

Figure 5 illustrates the strength of decadal-scale variations, (a) within one site (P3c), and (b) between the nine high-elevation sites in the Chaprot (P2b, P2c), Morkhun (P3a–P3d), Satpara (P4b, P4c) and the single-tree chronology from the Hunza valley (P5) in the Karakorum region since AD 1700. When comparing the 15 single series of site P3c, remarkably strong, synchronous decadal-scale variations are evident (Figure 5a; see also Table 1, Coeff. of var.). These decadal-scale variations are common in amplitude and persistence structure. They are also common among the nine high-elevation sites, even though these sites are separated by more than 100 km over the Karakorum region (Figure 5b). However, the strength of the decadal signal changes through time. For example, common decadal-scale variations are strong around 1800, but less coherent between 1825 and 1855.

The decadal signal has sufficient common strength to allow the calculation of a regional chronology, from the nine high-elevation sites in the Karakorum, for comparison with a corresponding regional chronology from the Tien Shan since AD 1258 (Figure 5c). Prior to 1258, the Tien Shan chronology has insufficient sample depth ($n = 3$ trees) for effective comparison. The overall correlation coefficient between the smoothed chronologies from the Karakorum and Tien Shan is $R_{(1258-1990)} = 0.4$.

Periods of synchronous and non-synchronous decadal fluctuations between the Karakorum and Tien Shan were evaluated. In the Karakorum region, between AD 1375 and 1475, the decadal signal is weak. Between AD 1475 and 1600, the growth response in the two regions is not equal. However, before 1375 and after 1600, strong synchronous decadal-scale variations are found in both regions. Even if marginal shifts in time or slight differences in amplitude occur, a reconstruction of decadal-scale variations from high-elevation sites in the Karakorum reflects similar decadal-scale variations found in the Tien Shan. In addition to the reconstruction of supraregional pointer years, this result provides further evidence for uniform growth variations in Western Central Asia.

Calibration of high-frequency and decadal-scale variations

High-frequency calibration analyses, based on monthly records of temperature and precipitation from six meteorological stations, display a complex pattern with TRW variations in the Karakorum. Many of the correlation coefficients are not strongly significant, a result that might be affected by less representative, low-elevation meteorological stations (Tessier, 1989). This becomes increasingly evident when annual averages of precipitation and temperature are used to calibrate TRW variations. Averaging the records of temperature and precipitation over the entire year reduces the noise of insufficient stations. The high-frequency variations of most high-elevation sites correlate significantly with mean annual temperature. For the Karakorum regional mean chronology, which is the average curve of nine sites located above 3500 m a.s.l., the correlation coefficient between tree growth and annual temperature is $R_{(1900-1975)} = 0.32$ (5% level of significance = 0.22).

Within the Tien Shan region, there is additional opportunity to validate TRW variations indirectly via an already calibrated MXD chronology of *Pinus tienschanica*, that records high-frequency July–August temperature variations (nearby Station Narin, $R_{(1886-1970)} = 0.81$) (Figure 6a). Using the MXD chronology as a proxy record of July–August temperature predictors, the TRW chronology of *Juniperus turkestanica* from site K1b is significantly correlated with Tien Shan summer temperature ($R_{(1886-1970)} = 0.35$).

Correlation coefficients, calculated with a windowing procedure over shorter intervals, indicate a significant decline of coherence during the last part ($R_{(1943-1970)} = -0.1$) of the entire proxy calibration period (Figure 6b). Increasing human disturbance since the 1940s might cause this decrease. However, the shown example additionally confirms the temperature dependence of high-elevation TRW chronologies in the Karakorum region. It also demonstrates the teleconnection between the Southern Tien Shan TRW sites and the high-latitude circumpolar MXD network (Briffa *et al.*, 1998a; 1998b).

Figure 7 shows the correlation between TRW decadal-scale variations and filtered annual temperature anomalies (dotted curve), measured at six meteorological stations since AD 1876. The recorded decadal-scale temperature fluctuations cause decadal-scale TRW variations that are exceptionally synchronous

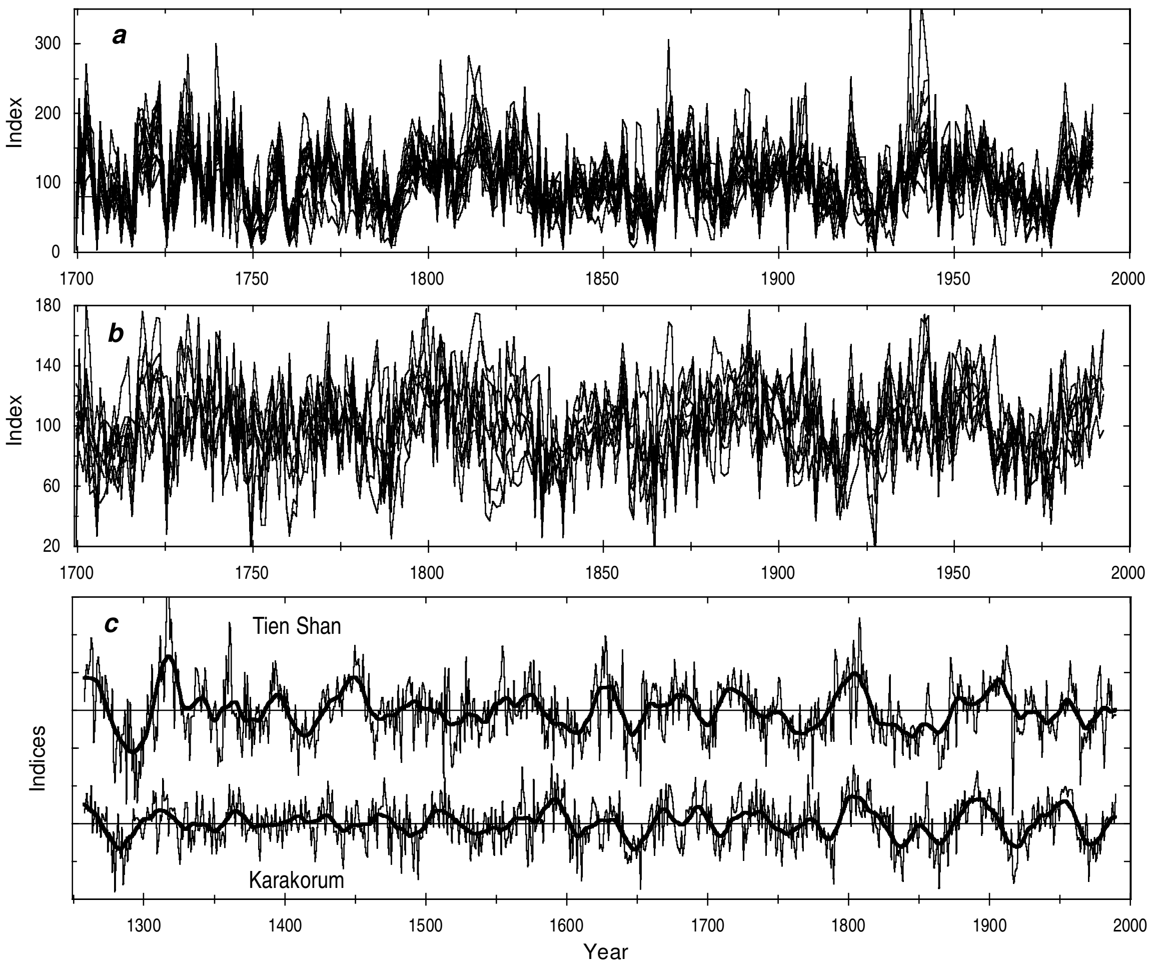

Figure 5 Verification of common decadal-scale TRW variations and comparison between the Karakorum and Tien Shan. (a) Observed TRW variations of the 15 standardized single series at site P3c (AD 1700–1990). (b) TRW variations of nine standardized mean chronologies from high-elevation sites above 3500 m a.s.l. in the Karakorum (1700–1990). (c) Comparison of the standardized regional chronology from the Karakorum versus the standardized regional chronology from the Tien Shan.

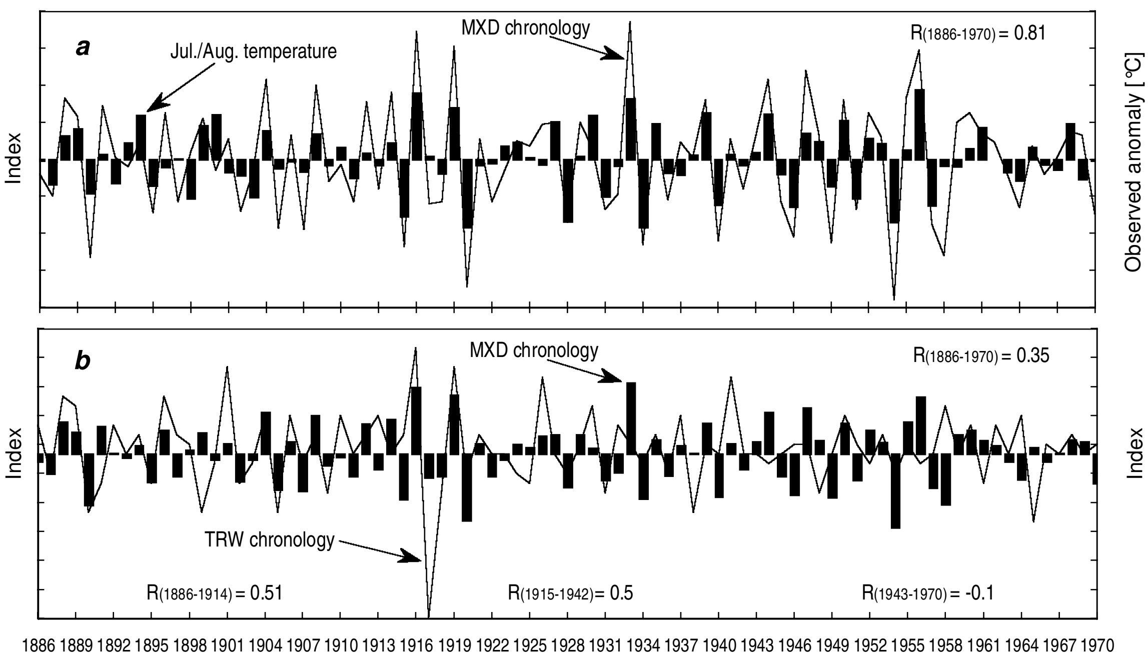

Figure 6 Example of high-frequency TRW calibration using MXD records as predictors. (a) The MXD chronology of *Pinus tienschanica* (solid curve) correlates well ($R = 0.81$) with July–August anomalies (columns), recorded at the station Narin for the period AD 1886–1970 (1% level of significance = 0.21). Tree site (41°40′N/76°26′E) and station (41°40′N/76°00′E) are located in Central Tien Shan. (b) The TRW chronology K1b of *Juniperus tienschanica* (solid curve), located in Southern Tien Shan, correlates well for the early ($R_{(1886-1914)} = 0.51$) and middle period ($R_{(1915-1942)} = 0.5$) with the MXD chronology (columns). In the most recent period, the correlation declines to zero ($R_{(1943-1970)} = -0.1$).

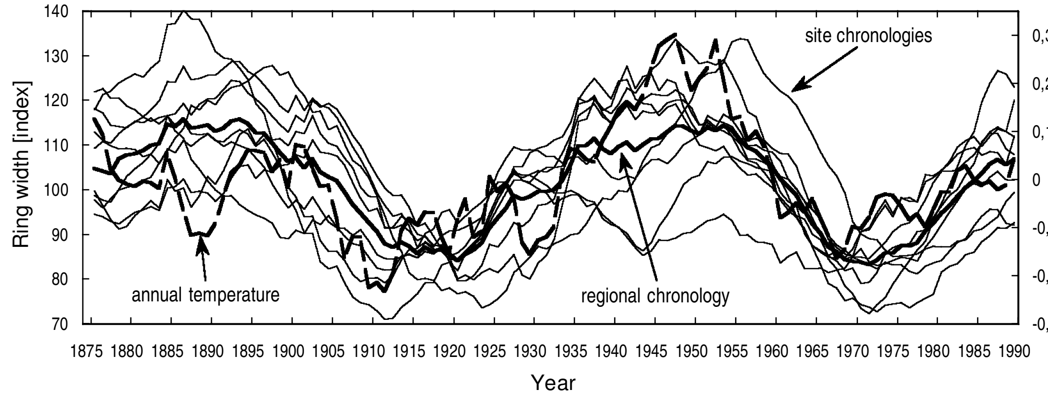

Figure 7 Calibration of decadal-scale TRW variations recorded at nine high-elevation sites distributed over the Karakorum region. Annual temperature anomalies (dotted curve) reflect the average of six meteorological stations. Decadal-scale variations of the site chronologies (thin curves), as well as the regional site average (bold curve) are forced by decadal-scale variations of annual temperature (regional chronology/temperature anomalies: $R_{(1876-1990)} = 0.63$ and $R_{(1900-1990)} = 0.76$). All series were smoothed to emphasize decadal-scale variations.

between the high-elevation sites of the Karakorum. The nine high-elevation TRW chronologies (thin curves) are distributed over several distant valleys. The regional chronology from these sites (bold curve) strongly correlates with recorded temperature anomalies for the entire period 1876–1990 ($R = 0.63$), and increases during the modern period ($R_{(1900-1990)} = 0.76$).

Independent calibration and verification leads to a linear transfer function y = 0,0073x – 0.746 ($R^2 = 0.434$) for the period 1876–1990. The observed decadal-scale TRW variations (where centennial trends have been removed) reflect 1200 years of temperature anomalies ranging between +0.2 and –0.2°C (see Figure 10). Further details on calibration, verification and reconstruction of decadal-scale variations are explained in Esper (2000b).

Centennial trends – 'Mediaeval Warm Period' and 'Little Ice Age'

Two different techniques were applied to describe the low-frequency trends. First, the overall trend of 97 single TRW juniper series, all over 500 years old, from both the Karakorum and Tien Shan regions is discussed (Figure 8). Second, the low-frequency trends of a subset of 17 juniper trees, all over 1000 years old, from the Karakorum region are analysed (Figure 9).

Long-term growth trends of 97 juniper series, shown as smoothed, 101-year kernel low-pass filters fluctuating around the average growth (Figure 8, vertical axis = 0), indicate periods of high and low overall growth. In Figure 8, three distinct periods, AD 901–1100 (a), AD 1601–1800 (b) and the twentieth century (c), have been selected. Between AD 901 and 1100 ($n = 200$ years), 81.6% of all TRW values lie above the long-term average of the entire series. The remaining, less than 20% of the values, fall short of the average or are close to zero. That means most of the juniper trees grew better around AD 1000 than the long-term average, while only a few of these series seem to be biased by age-related trends (top of Figure 8). Additionally, around AD 1000 most of the series show no negative trends, and several trends are positive. Another feature that points to broadly missing, biasing, age-related effects is the increasing TRW values in the most recent period of the record.

Between AD 1601 and 1800 ($n = 200$ years), 70.5% of all values exhibit growth rates below the average. In this period many of the trees experienced extraordinarily high stress. Finally, between AD 1901 and 1990, the ratio of TRW values above/below average returns to parity. Following these criteria of observed long-term growth anomalies, the trees of Western Central Asia show wide TRW around AD 1000 and narrow TRW around AD 1700. Overall growth in the twentieth century is then slightly above the long-term mean again.

The *ad*-indexed TRW series of 17 long-lived, high-elevation *Juniperus turkestanica* trees from the Karakorum region also display distinct periods of common growth trends since AD 618 (sample depth at AD 618 = four trees, Figure 9). Between AD 900 and 1000 tree growth was exceptionally rapid, at rates that cannot be observed during any other period of the last millennium.

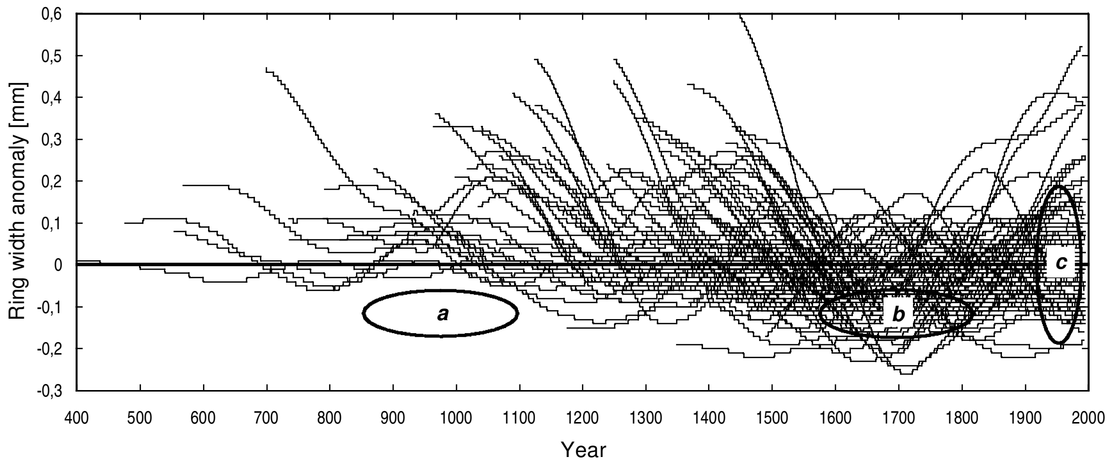

Figure 8 Kernel-filtered single series of 97 juniper trees, all over 500 years old. All series have been related to their long-term average, so that the TRW anomalies appear in mm. (a) Around AD 1000, most trees are growing above the long-term average. (b) Around AD 1700, the majority of trees are growing below the long-term average. (c) In the twentieth century, the ratio of above to below average growth returns to parity again.

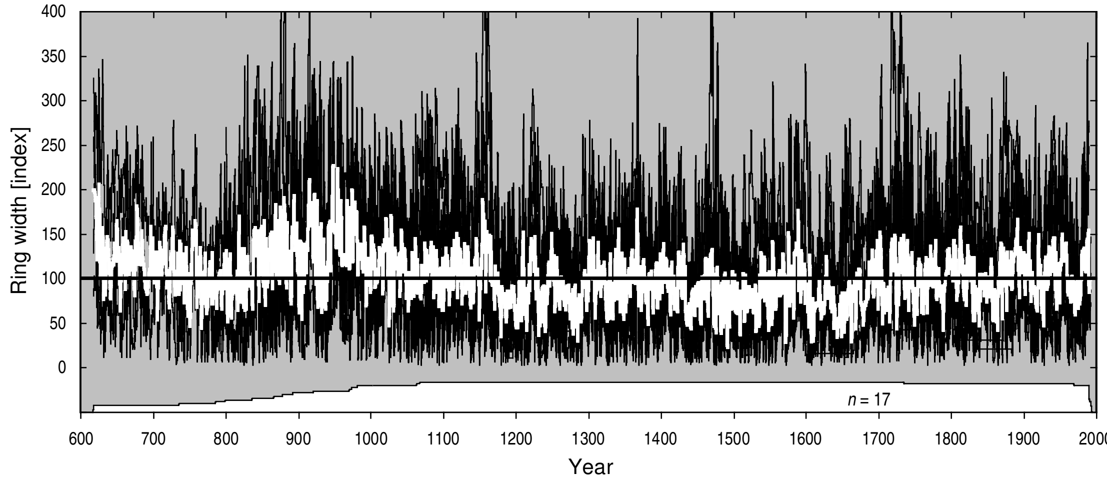

Figure 9 Centennial trends of 17 long-lived *Juniperus turkestanica* trees from several high-elevation sites, distributed over the Karakorum region, since AD 618. All series were standardized by calculating ratios from the average growth rates of the individual series. The white band in the centre indicates the mean curve of all single series.

Between AD 1000 and 1200, a trend towards poorer growing conditions was recorded. At about AD 1500, minimum TRW values are reached, persisting well into the seventeenth century. Towards the twentieth century, TRW values increase again. However, the twentieth-century trend does not approach the AD 1000 maximum. These long-term trends starting in the early seventh century – reflecting the 'Mediaeval Warm Period', 'Little Ice Age' and recent warming – can be emphasized by calculating a kernel low-pass filter (Gasser and Müller, 1984), as illustrated in Figure 10 (shaded planes).

Some remarks on the observed centennial trends need to be mentioned. (1) The observed decadal-scale variations of the 17 trees (Figure 9) are better represented in Figure 5. (2) Because of the characteristic growth forms, population density and standardization technique, changes in sample depth, as shown at the bottom of Figure 9, do not affect growth trends in the early period of the reconstruction. A decreasing trend after AD 700 clearly demonstrates the absence of age-related bias in the later periods. (3) Centennial trends in TRW cannot be calibrated with instrumental records of 100 years length. However, the strength of the climatic signal at interannual, as well as decadal, scales suggests that temperature also forces centennial fluctuations.

Climate history since AD 618

This paper represents a synopsis of climatically forced TRW variations, combining three separated frequencies – interannual-, decadal- and centennial-scale variations – into a comprehensive reconstruction of Western Central Asian climate since AD 618 (Figure 10). So far, the discussion of the distinct wavelengths has been carried out independently. Now it is essential to reunite the three frequencies.

Climate history in Western Central Asia is determined by centennial trends, indicating above-average conditions until AD 1139. Since AD 1140, growth is reduced below the long-term average of the last 1373 years decreasing further well into the sixteenth century. Since the seventeenth century, an increase of TRW values is observed, which intersects the long-term mean in 1875. Growing conditions in the twentieth century exceed the long-term average, but the amplitude of this trend is not comparable to the conditions around AD 1000 (Figure 10, shaded planes).

Superimposed on the centennial wavelength is the decadal variability. The decadal fluctuations highlight temperature-forced variations within a range of –0.2 to +0.2°C. Note that the illustrated amplitudes of decadal- and centennial-scale variations in Figure 10 are not related to each other. After AD 790, decadal-

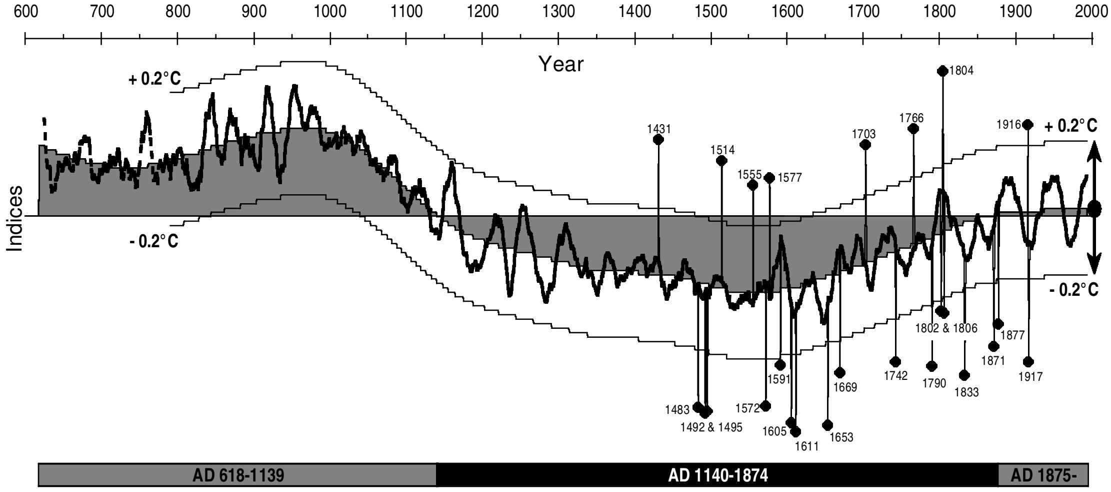

Figure 10 Western Central Asia climate variations since AD 618. The synopsis of centennial trends (shaded planes), decadal-scale variations (solid curve) and supraregional pointer years (diamonds and dates) leads to a comprehensive reconstruction of climate variability. The dotted curve indicates the early decadal-scale variations observed by 17 long-lived *Juniperus turkestanica* trees. The illustrated amplitudes of the separated frequencies are not related to each other in terms of direct comparability.

scale variations have been recorded at nine high-elevation sites of the Karakorum region (Figure 10, bold curve), and before AD 790 it appears in only 17 long-lived juniper trees (dotted curve).

Finally, the record of supraregional pointer years, which occur synchronously in both Karakorum and Tien Shan, completes the reconstruction (Figure 10, diamonds and dates). Again, the amplitude of the pointer years displayed is not related to the centennial trends or the –0.2/+0.2 temperature range. However, it may be assumed that in each period since AD 618 pointer years significantly exceeded the illustrated decadal temperature range.

Discussion and conclusion

A prolonged centennial trend towards better growing conditions has been observed over the last *c.* 300 years in the Western Central Asia tree-ring records. This trend is of a lesser magnitude compared with conditions before *c.* AD 1100. This result indicates the existence of a 'Mediaeval Warm Period', as well as a recent trend of warming, similar to that documented from other areas of the Northern Hemisphere (e.g., Flohn, 1988; Lamb, 1977; 1982; see also critical remarks by Hughes and Diaz, 1994). These positive anomalies are separated by a prolonged period of poor growth, which reflects the 'Little Ice Age' in Western Central Asia. Even though this wavelength cannot seriously be calibrated using records of instrumental climate data, centennial-scale variations seem to be forced predominantly by temperature variations. Besides the comparison with long proxy reconstructions from elsewhere (Esper, 2000b), a strong temperature forcing, producing remarkable high amounts of common, decadal-scale variations at high-elevation sites of Western Central Asia, supports the hypothesis of temperature-induced centennial-scale variations. To give a comprehensive synopsis of climate history in Western Central Asia, the reconstructed decadal-scale variations, as well as the supraregional pointer years, need to be added to the centennial trends. Decadal fluctuations vary within the range of –0.2 to +0.2°C. The warmest decades since AD 618 appear between AD 800 and 1000, whereas the coldest periods were recorded in the first half of seventeenth century.

The reconstructed supraregional pointer years and the decadal fluctuations need to be integrated in a Central Asia network (Bräuning, 1994; 1999; Graybill *et al.*, 1992; Hughes, 1992; Jacoby *et al.*, 1996; Ramesh *et al.*, 1985; Xiangding and Xuemei, 1995; Yadav *et al.*, 1997; Zimmermann *et al.*, 1997). Cross-dating of extreme growth reactions might be the first step towards the implementation of a region-wide network. Initial comparisons verified remarkable linkages to the high-latitude circumpolar MXD network (Briffa *et al.*, 1998a; 1998b; Schweingruber and Briffa, 1996).

Acknowledgements

This study was supported by the DFG (German Science Foundation, DFG grant No. Wi-937–1/5) within the framework of the CAK project (Culture Area Karakorum). We thank P.J. Krusic, K.R. Briffa, R. D'Arrigo, H. Gärtner, P.D. Jones, J. Nagel, B. Neuwirth and K. Treydte for valuable comments and criticisms on earlier drafts of this paper.

References

Barnett, T.P., Dümenil, L., Schlese, U. and **Roeckner, E.** 1988: The effect of Eurasian snow cover on global climate. *Science* 239, 504–507.

Böhner, J. 1996: Säkulare Klimaschwankungen und rezente Klimatrends Zentral- und Hochasiens. *Göttinger Geographische Abhandlungen* 101.

Bräker, O.U. 1981: Der Alterstrend bei Jahrringdichten und Jahrringbreiten von Nadelhölzern und sein Ausgleich. *Mitteilungen der Forstlichen Bundesversuchsanstalt Wien* 142, 75–102.

Bräuning, A. 1994: Dendrochronology for the last 1400 years in Eastern Tibet. *GeoJournal* 34, 75–95.

—— 1999: Zur Dendroklimatologie Hochtibets während des letzten Jahrtausends. *Dissertationes Botanicae* 312.

Briffa, K.R. and **Jones, P.D.** 1990: Basic chronology statistics and assessment. In Cook E.R. and Kairiukstis, L.A., editors, *Methods of dendrochronology: applications in the environmental science*, Dordrecht: Kluwer/IIASA, 137–52.

Briffa, K.R. and **Osborn, T.J.** 1999: Seeing the wood from the trees. *Science* 284, 926–27.

Briffa, K.R., Jones, P.D., Schweingruber, F.H., Karlén, W. and **Shiyatov, S.** 1996: Tree-ring variables as proxy-climate indicators: problems with low-frequency signals. In Jones, P.D., Bradley, R.S. and Jouzel, J., editors, *Climatic variations and forcing mechanisms of the last 2000 years*, Berlin: Springer, 9–41.

Briffa, K.R., Jones, P.D., Schweingruber, F.H., Shiyatov, S. and **Cook, E.R.** 1995: Unusual twentieth-century summer warmth in a 1000-year temperature record from Siberia. *Nature* 376, 156–59.

Briffa, K.R., Jones, P.D., Schweingruber, F.H. and **Osborn, T.J.** 1998a: Influence of volcanic eruptions on Northern Hemisphere summer temperature over the past 600 years. *Nature* 393, 450–54.

Briffa, K.R., Schweingruber, F.H., Jones, P.D., Osborn, T.J., Shiyatov, S.G. and **Vaganov, E.A.** 1998b: Reduced sensitivity of recent tree-growth to temperature at high northern latitudes. *Nature* 391, 678–82.

Cook, E.R. and **Briffa, K.** 1990: A comparison of some tree-ring standardization methods. In Cook, E.R. and Kairiukstis, L.A., editors, *Methods of dendrochronology: applications in the environmental science*, Dordrecht: Kluwer/IIASA, 153–62.

Cook, E.R. and **Kairiukstis, L.A.** 1990: *Methods of dendrochronology: applications in the environmental science*. Dordrecht: Kluwer/IIASA.

Cook, E.R. and **Peters, K.** 1997: Calculating unbiased tree-ring indices for the study of climatic and environmental change. *The Holocene* 7, 361–70.

Cook, E.R., Briffa, K.R., Meko, D.M., Graybill, D.A. and **Funkhouser, G.** 1995: The 'segment length curse' in long tree-ring chronology development for palaeoclimatic studies. *The Holocene* 5, 229–37.

Cook, E.R., Briffa, K., Shiyatov, S. and **Mazepa, V.** 1990. Tree-ring standardization and growth trend estimation. In Cook, E.R. and Kairiukstis, L.A., editors, *Methods of dendrochronology: applications in the environmental science*, Dordrecht: Kluwer/IIASA, 104–23.

Cropper, J.P. 1979: Tree-ring skeleton plotting by computer. *Tree-Ring Bulletin* 39, 47–59.

Dean, J.S., Meko, D.M. and **Swetnam, F.W.**, editors, 1996: *Tree rings, environment and humanity: proceedings of the international conference, Tucson, Arizona, 17–21 May 1994.* Tucson: Radiocarbon.

Esper, J. 2000a: Long-term tree-ring variations in *Juniperus* at the upper timber-line in the Karakorum (Pakistan). *The Holocene* 10, 253–60.

——. 2000b: Paläoklimatische Untersuchungen an Jahrringen im Karakorum und Tien Shan Gebirge (Zentralasien). *Bonner Geographische Abhandlungen* 103.

Esper, J., Bosshard, A., Schweingruber, F.H. and **Winiger, M.** 1995: Tree-rings from the upper timberline in the Karakorum as climatic indicators for the last 1000 years. *Dendrochronologia* 13, 79–88.

Esper, J., Neuwirth, B. and **Treydte, K.** 2001: A new parameter to evaluate temporal signal strength of tree ring chronologies. *Dendrochronologia* 19, 93–102.

Ferguson, C.W. 1968: *Bristlecone pine*: science and esthetics. *Science* 159, 839–46.

Flohn, H. 1958: Beiträge zur Klimakunde von Hochasien. *Erdkunde* 12, 294–308.

——. 1988: *Das Problem der Klimaänderungen in Vergangenheit und Zukunft.* Darmstadt: Wissenschaftliche Buchgesellschaft.

Fritts, H.C. 1969: Bristlecone pine in the White Mountains of California: growth and ring-width characteristics. *Papers of the Laboratory of Tree-ring Research* 4.

——. 1976: *Tree rings and climate*. London: Academic Press.

Gasser, T. and **Müller, H.G.** 1984: Estimating regression function and their derivatives by the kernel method. *Scandinavian Journal of Statistics* 11, 171–85.

Graybill, D.A. and **Idso, S.B.** 1993: Detecting the aerial fertilization effect of atmospheric CO_2 enrichment in tree-ring chronologies. *Global Biochemical Cycles* 7, 81–95.

Graybill, D.A., Shiyatov, S.G. and **Burmistrov, V.F.** 1992: Recent dendrochronological investigations in Kirghizia, USSR. In Bartholin, T.S., Berglund, B.E., Eckstein, D. and Schweingruber, F.H., editors, *Tree rings and environment*, Lundqua report 34, 123–27.

Hughes, M.K. 1992: Dendroclimatic evidence from the Western Himalaya. In Bradley, R.S. and Jones, P.D., editors, *Climate since* AD *1500*, London: Routledge, 415–31.

Hughes, M.K. and **Diaz, H.F.** 1994: Was there a 'Medieval Warm Period', and, if so, where and when? *Climatic Change* 26, 109–42.

Ives, J.D. and **Messerli, B.** 1989*: The Himalayan dilemma: reconciling development and conservation.* London: Routledge.

Jacoby, G.C., D'Arrigo, R.D. and **Davaajamts, T.** 1996: Mongolian tree rings and 20th-century warming. *Science* 273, 771–73.

Jones, P.D., Bradley, R.S. and **Jouzel, J.**, editors, 1996: *Climatic variations and forcing mechanisms of the last 2000 years*. Berlin: Springer.

Kelly, P.E., Cook, E.R. and **Larson, D.W.** 1992: Constrained growth, cambial mortality, and dendrochronology of ancient *Thuja occidentalis* on cliffs of the Niagara Escarpment – an eastern version of bristlecone pine? *International Journal of Plant Science* 153, 117–27.

La Marche, V.C. 1974: Paleoclimatic inferences from long tree-ring records. *Science* 183, 1043–48.

Lamb, H.H. 1977: *Climate, present, past and future*, volume 2. London: Methuen.

——. 1982: *Climate, history and the modern world.* London: Methuen.

Mann, E.M., Bradley, R.S. and **Hughes, M.K.** 1998: Global-scale temperature patterns and climate forcing over the past six centuries. *Nature* 392, 779–87.

Nüsser, M. 1998: Nanga Parbat (NW-Himalaya): Naturräumliche Ressourcenausstattung und humanökologische Gefügemuster der Landnutzung. *Bonner Geographische Abhandlungen* 97.

Ramesh, R., Bhattacharyya, S.K. and **Gopalan, K.** 1985: Dendroclimatological implications of isotope coherence in trees from Kashmir Valley, India. *Nature* 317, 802–804.

Reimers, F. 1992: Untersuchungen zur Variabilität der Niederschläge in den Hochgebirgen Nordpakistans und angrenzender Gebiete. *Beiträge und Materialien zur Regionalen Geographie* 6.

Schickhoff, U. 1993: Das Kaghan–Tal im Westhimalaya (Pakistan). *Bonner Geographische Abhandlungen* 87.

—— 1995: Verbreitung, Nutzung und Zerstörung der Höhenwälder im Karakorum und in angrenzenden Hochgebirgsräumen Nordpakistans. *Petermanns Geographische Mitteilungen* 139, 67–85.

Schweinfurth, U. 1956: Über klimatische Trockentäler im Himalaya. *Erdkunde* 10, 297–302.

Schweingruber, F.H. 1996: *Tree rings and environment: dendroecology.* Bern: Haupt.

Schweingruber, F.H. and **Briffa, K.R.** 1996: Tree-ring density networks for climate reconstruction. In Jones, P.D., Bradley, R.S. and Jouzel, J., editors, *Climatic variations and forcing mechanisms of the last 2000 years*, Berlin: Springer, 43–66.

Schweingruber, F.H., Eckstein, D., Serre-Bachet, F. and **Bräker, O.U.** 1990: Identification, presentation and interpretation of event years and pointer years in dendrochronology. *Dendrochronologia* 8, 9–38.

Schweingruber, F.H., Wehrli, U., Aellen-Rumo, K. and **Aellen, M.** 1991: Weiserjahre als Zeiger extremer Standorteinflüsse. *Schweizer Zeitschrift für Forstwesen* 142, 33–52.

Shiyatov, S.G. 1993: The upper timberline dynamics during the last 1100 years in the Polar Ural Mountains. In Frenzel, B., editor, Oscillations of the alpine and polar tree limits in the Holocene, *Paläoklimaforschung – Palaeoclimate Research* 9, Stuttgart: Gustav Fischer, 195–203.

Tessier, L. 1989: Spatio-temporal analysis of climate-tree ring relationship. *The New Phytologist* 111, 517–29.

Troll, C. 1952: Die Lokalwinde der Tropengebirge und ihr Einfluβ auf Niederschlag und Vegetation. *Bonner Geographische Abhandlungen* 9, 124–82.

Vaganov, E.A., Hughes, M.K., Kirdyanov, A.V., Schweingruber, F.H. and **Silkin, P.P.** 1999: Influence of snowfall and melt timing on tree growth in subarctic Eurasia. *Nature* 400, 149–51.

Weiers, S. 1995: Zur Klimatologie des NW-Karakorum und angrenzender Gebiete. Statistische Analysen unter Einbeziehung von Wettersatellitenbildern und eines Geographischen Informationssystems (GIS). *Bonner Geographische Abhandlungen* 92.

—— 1998: Wechselwirkungen zwischen sommerlicher Monsunaktivität und auβertropischer Westzirkulation in den Hochgebirgsregionen Nordpakistans. *Petermanns Geographische Mitteilungen* 142, 85–104.

Wigley, T.M.L., Briffa, K.R. and **Jones, P.D.** 1984: On the average of correlated time series, with applications in dendroclimatology and hydrometeorology. *Journal of Climate and Applied Meteorology* 23, 201–13.

Wright, R.D. and **Mooney, H.A.** 1965: Substrate-oriented distribution of bristlecone pine in the White Mountains of California. *The American Midland Naturalist* 73, 257–84.

Xiangding, W. and **Xuemei, S.** 1995: Status and prospects of dendrochronological study in Tibetan Plateau. *Dendrochronologia* 13, 89–98.

Yadav, R.R., Park, W.K. and **Bhattacharyya, A.** 1997: Dendroclimatic reconstruction of April–May temperature fluctuations in the Western Himalaya of India since AD 1698. *Quaternary Research* 48, 187–91.

Zimmermann, B., Schleser, G.H. and **Bräuning, A.** 1997: Preliminary results of a Tibetan stable C-isotope chronology dating from 1200 to 1994. *Isotopes in Environmental and Health Studies* 33, 157–65.